

ESA STUDY CONTRACT REPORT –

Deliverable D 3.1

Mechanical tests and NDT evaluation – technical note

ESA Contract No: 400114452/15/ NL/NDe	SUBJECT: Milestone 3, D 3.1 Specimen manufacturing and NDT evaluation – technical note	CONTRACTOR: Riga Technical University, Institute of Materials and Structures
* ESA CR()No:	No. of Volumes:1 This is Volume No:1	CONTRACTOR'S REFERENCE: 62518 (bidder code)
ABSTRACT: The aim of current deliverable/technical note is to summarize initial work towards prototyping of CFRP/Al-honeycomb sandwich panel manufacturing, and prototyping practice in line with NDT evaluation and characterisation of obtained specimens. The work has focused on thin wall CFRP plate production with aim to reduce thickness distribution variety and to obtain “almost” no porosity specimens as one relevant to autoclave production. A next step was to focus on honeycomb extrusion and adhesion with CFRP skins for panel production. Finally, NDE by means of ultrasound A, B and C scans have been performed and statistical distribution of obtained quality have been investigated. In addition, NDT by means of physical self-frequency measurements was performed to have a second means of quality assurance of both – CFRP skins and CFRP/Al honeycomb panels.		
The work described in this report was done under ESA Contract. Responsibility for the contents resides in the author or organisation that prepared it.		
Names of authors: Kaspars Kalniņš; Guntis Japiņš; Eduards Skuķis; Oļģerts Ozoliņš.		
** NAME OF ESA STUDY MANAGER: DIV: DIRECTORATE:	** ESA BUDGET HEADING:	

Table of contents

1	Introduction.....	3
2	Sample manufacturing.....	3
2.1	Face skin manufacturing strategies	3
2.2	Face skin prototyping	3
2.3	Face skin panel manufacturing.....	8
2.4	Honeycomb preparation	18
2.5	Panel assembly	22
3	Experimental procedures.....	22
3.1	Non-destructive testing – Modal assurance criterion	24
3.1.1	Introduction to Modal assurance criterion	24
3.1.2	Modal Assurance Criterion presentation formats	24
3.1.3	Modal Assurance Criterion (MAC) Zero.....	25
3.1.4	Modal Assurance Criterion (MAC) Unity.	25
3.1.5	Experimental procedure and results	25
3.1.6	Conclusions	27
4	References	28

1 Introduction

Interim report on manufacturing procedures and non-destructive inspections gives a brief overview on preliminary studies on sandwich CFRP skin and CFRP/Al honeycomb manufacturing aspects, manufacturing and testing of test fixtures designed for specific test procedures, development of non-destructive techniques for component quality control and measurement of realized material imperfections as well as introduced damage imperfections (CAI).

2 Sample manufacturing

2.1 Face skin manufacturing strategies

Four different skin-manufacturing techniques were employed during current study. Two approaches were considered as atmospheric pressure (vacuum bagging) compaction and two were mechanically compacted (non-vacuum bagged). All four approaches used oven for curing of pre-preg laminate. All skin samples were considered as minimal thickness symmetrical lay-up, consisting of only three layers ($0^0/90^0/0^0$), except one specimen considering just two cross ply layers. Two areal weight pre-pregs 100 g/m^2 and 200 g/m^2 , were selected. Properly compacted and cured lay-up consisting of at least three plies produces average ply thickness of 0.09 mm (for 100 g/m^2 pre-preg) and 0.15 mm (for 200 g/m^2 pre-preg).

Since pre-preg system used in the current study has waiving (non-uniform fibre spread) across the pre-preg sheet width, cross-ply laminate structure ($0^0/90^0$) stack, has some kind of net pattern formed by thicker portions of pre-preg sheet crossing the same features of overlaying ply. That's mean, that good compaction needed to help flatten those pre-preg thickness imperfections and form uniform thickness skin plate. Inadequate pressure introduced on the caul plates during curing cycle will introduce low-pressure areas (pockets), which collect entrapped air and form areas with high porosity.

Ambient atmospheric compaction approach employing vacuum bagging and outside atmospheric pressure to compact laminate lay-up. Furthermore, two different thickness caul plates were used to form uniform laminate surface. Where 2 mm thick aluminium caul plate showed adequate stiffness to avoid local defects caused by vacuum port pressure and edge bending etc. On the other hand, very thin 0.5 mm aluminium caul plate showed insufficient local stiffness, allowing appearing those indents on surface of CFRP plates. In both cases, an atmospheric pressure does not deliver satisfactory compaction needed to remove entrapped interlaminar air and minimize defects associated with entrapped air voids.

Mechanically compressed compaction approach facilitates compression of the pre-preg lay-up placed between two metal plates and compressed by means of mechanical clamps, introducing equal to 3-bar pressure that partly match autoclave curing.

2.2 Face skin prototyping

Ultrasound NDT inspections were introduced for all preliminary skin samples for quality control and thickness distribution measurements across the panel. Void distribution as well as thickness distribution of each individual panel summarized and presented in Figure 2.1. to Figure 2.8.

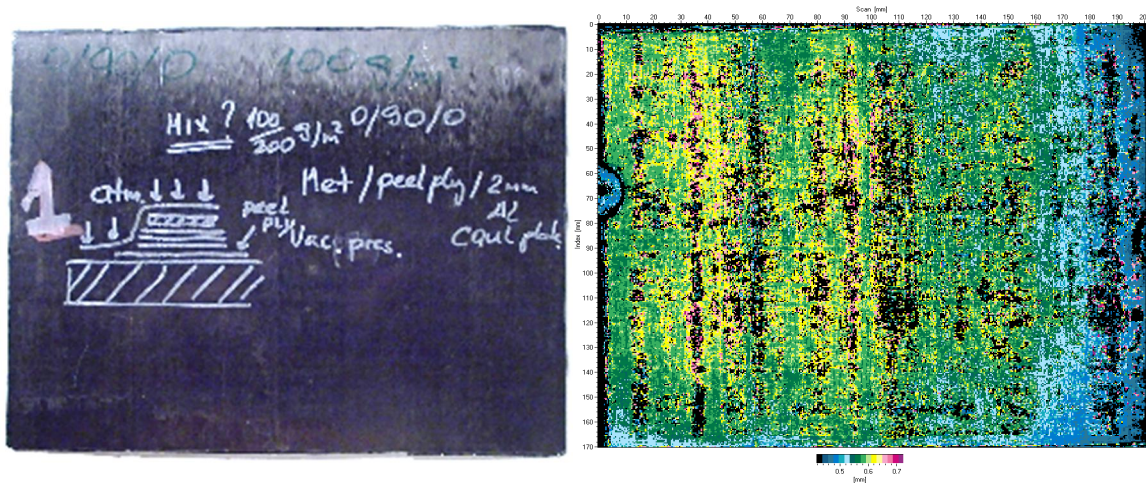


Figure 2.1. Panel I with corresponding US thickness scan

Specimen I represents three 0/90/0 layer CFRP panel compressed by atmospheric pressure (vacuum bag) with 2 mm aluminium caul plate at the top and peel ply at the bottom. NDT scan showed relatively good thickness distribution across the panel, but relatively poor compaction, causing void bands (black rows, see Figure 2.1.).

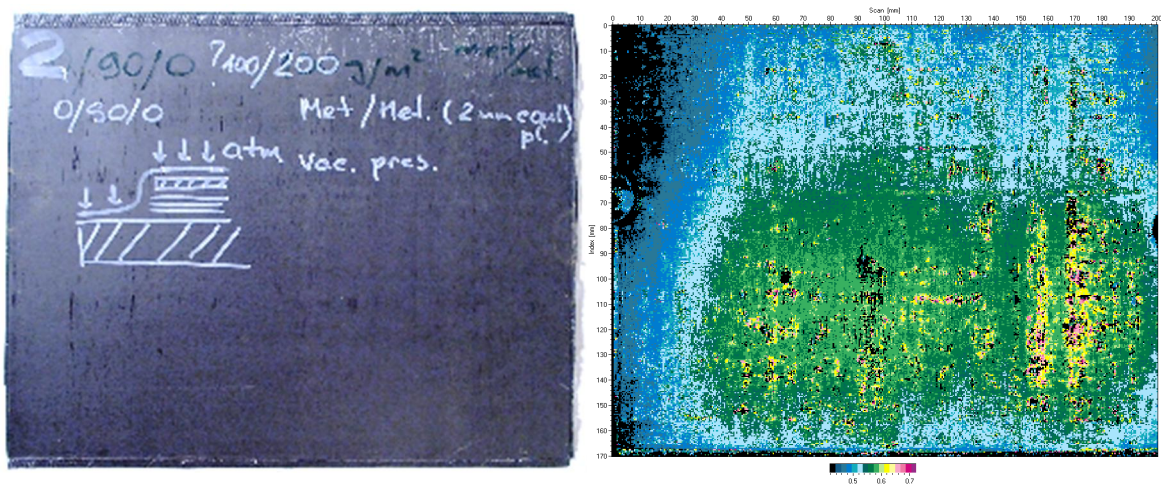


Figure 2.2 Panel II with corresponding US thickness scan

Specimen II represents three layer (possibly mixed 100 g/m² and 200 g/m²) panel compressed by atmospheric pressure (vacuum bag) with 2 mm aluminium caul plate at the top. NDT scan showed relatively good thickness distribution across the panel, but relatively poor compaction, showing void bands (black rows, see Figure 2.2.).

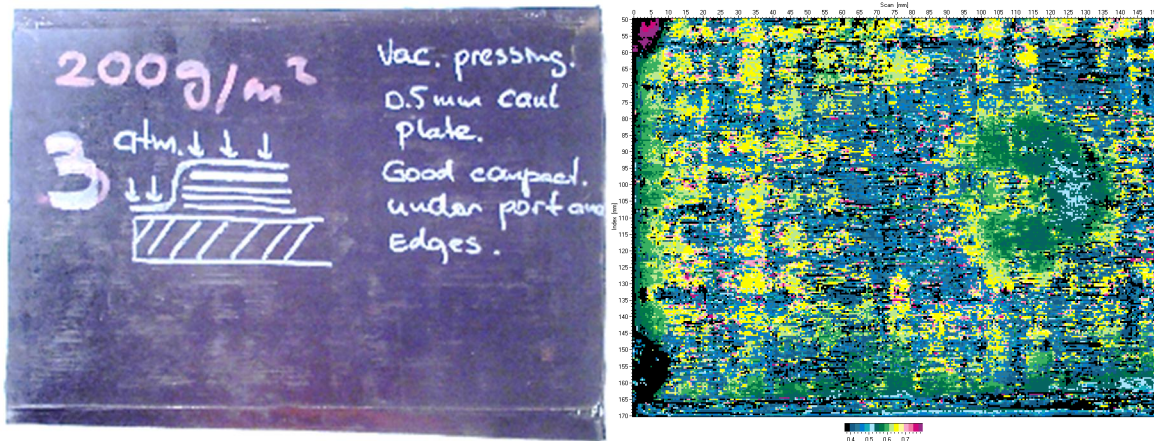


Figure 2.3. Panel III with corresponding US thickness scan

Specimen III represents three layer (200 g/m^2) panel compressed by atmospheric pressure (vacuum bag) with 0.5 mm aluminium caul plate at the top. NDT scan showed relatively good thickness distribution across the panel, poor compaction, a bit better along the caul plate edges and vacuum port (green colour, round footprint on right part of image), showing void bands across all the panel (black rows, see Figure 2.3.). It should be noted that thin caul plate eliminate voids caused by bridging of the different thickness pre-preg ply, which was especially most obvious with cross ply laminate, angle ply laminates possibly can be less affected, while UD laminates will eliminate this pre-preg faults completely. With the increase of laminate thickness this side effects eliminates too.

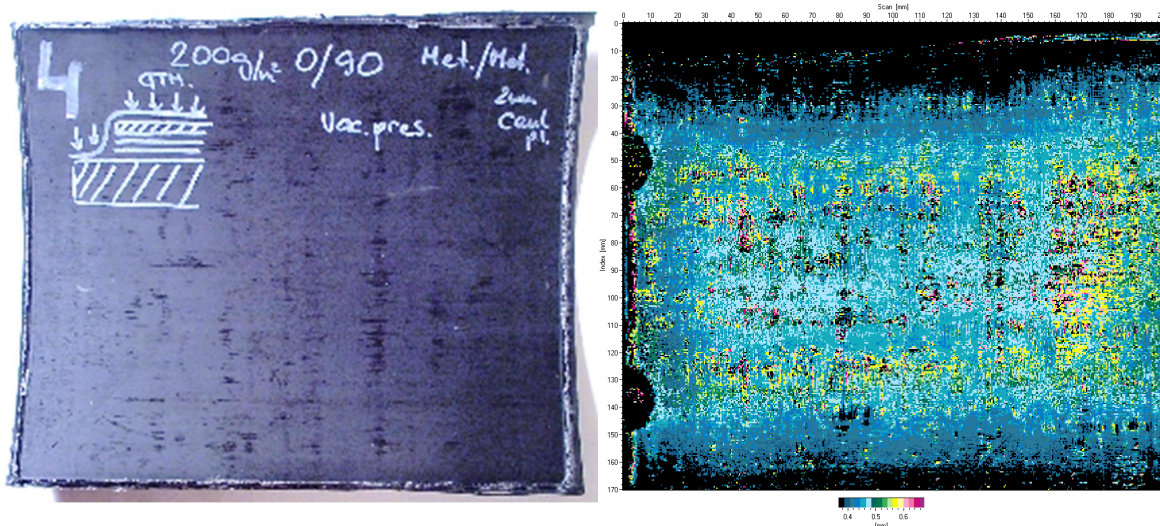


Figure 2.4. Panel IV with corresponding US thickness scan

Specimen IV represents two layer (200 g/m^2) panel compressed by atmospheric pressure (vacuum bag) with 2 mm aluminium caul plate at the top. NDT scan showed relatively good thickness distribution across the panel, poor compaction, showing void bands across the entire panel (black rows, see Fig.4). It should be noted that black band along two edges not indicate any failure, but showed-up due out of range scanning, caused by panel bending due to unsymmetrical layup (0/90).

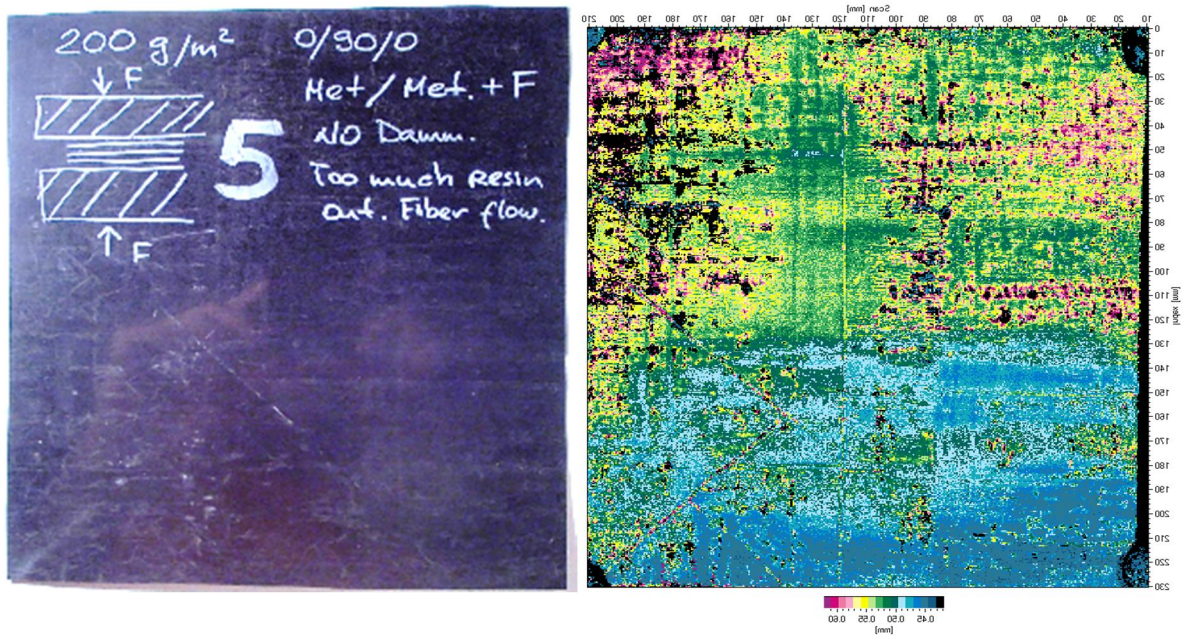


Figure 2.5. Panel V with corresponding US thickness scan

Specimen V represents three layer (200 g/m^2) panel compressed by pressure clamps (no vacuum bag applied for debulking), thick steel caul plates at the top and bottom were used. Laminate was placed between steel plates without dam, so too much resin loss and fibre flow was observed. NDT scan showed relatively good thickness distribution across the panel, still poor compaction (possibly associated with resin loss), some definite thickness difference, splitting panel horizontally in the middle (possibly associated with some thickness drop within single pre-preg layer or even multiplying (overlying) of those faults over two 0 layers, void bands showed across all the panel (black rows, see Figure 2.5.).

Specimen 6 represents three layer (100 g/m^2) panel compressed by pressure clamps (no vacuum bag applied for debulking), thick steel caul plates at the top and bottom were used. Laminate was placed between steel plates with dam formed by vacuum putty, so there are not resin loss and fibre flow was observed, but another side effect appeared, fibre wrinkling along 0 layer edges (can be associated with buckling of fibres due to expansion of dam inside the layup initial geometry during flow phase of resin (at 80°C)). NDT scan showed relatively good thickness distribution across the panel, poor compaction (possibly associated with dam stiffness); void bands showed across the entire panel (black rows, see Figure 2.6.).

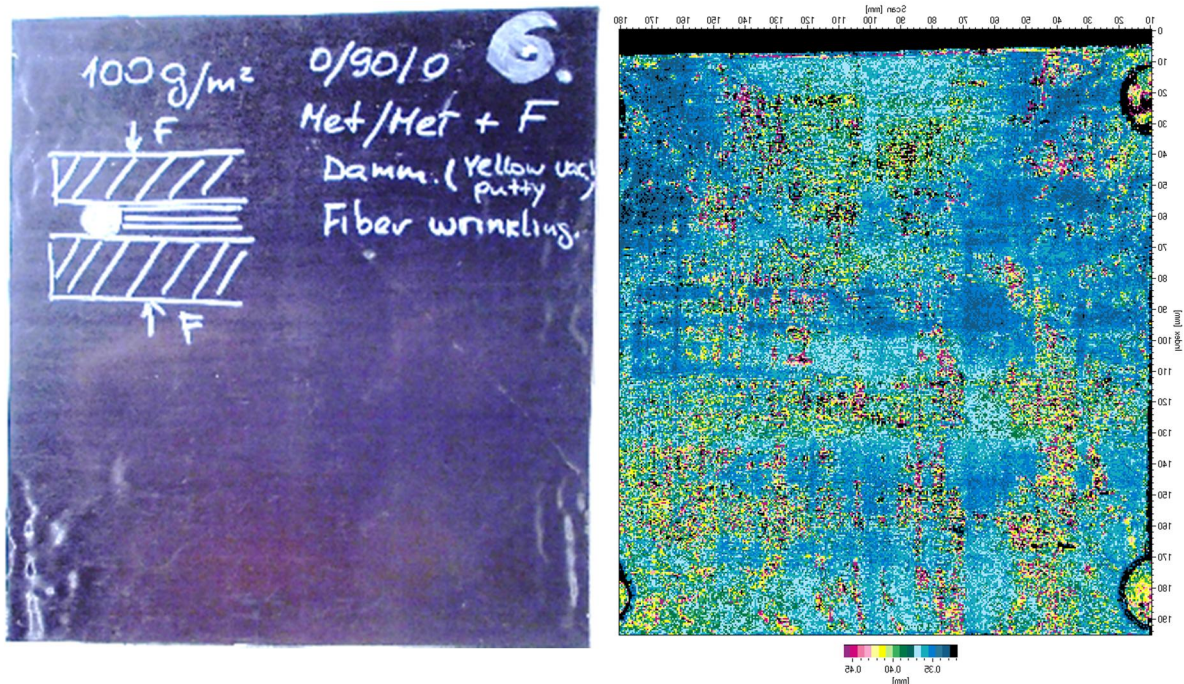


Figure 2.6. Panel VI with corresponding US thickness scan

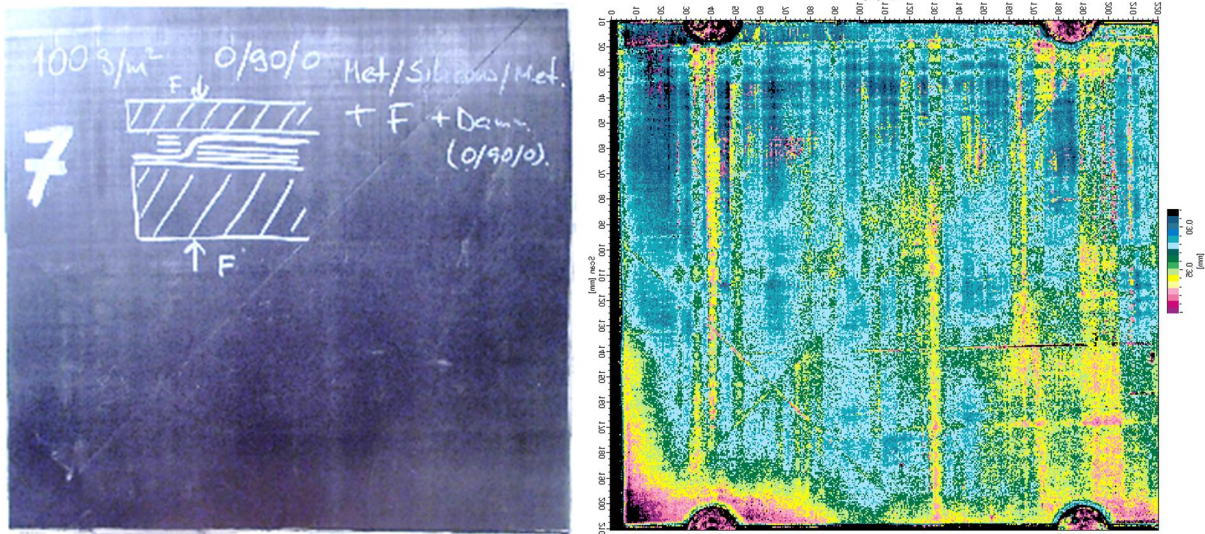


Figure 2.7. Panel VII with corresponding US thickness scan

Specimen VII represents three layer (100 g/m^2) panel compressed by pressure clamps (no vacuum bag applied for debulking), thick steel caul plates at the top and bottom were used. 1 mm silicon film layer were placed between upper caul plate and laminate with the reason to eliminate fibre bridging. Laminate was placed between steel plates, with dam formed by the same lay-up pre-preg 5 – 7 mm ribbons cut from the same panel. It should be noted that dam pre-preg ribbons was placed on the outside of the silicon film, so small amount of resin loss was observed. NDT scan showed good thickness distribution across the panel (except different thickness strips associated with pre-preg layer thickness variation), good compaction was observed, void spots was eliminated across the entire panel (see Figure 2.7.).

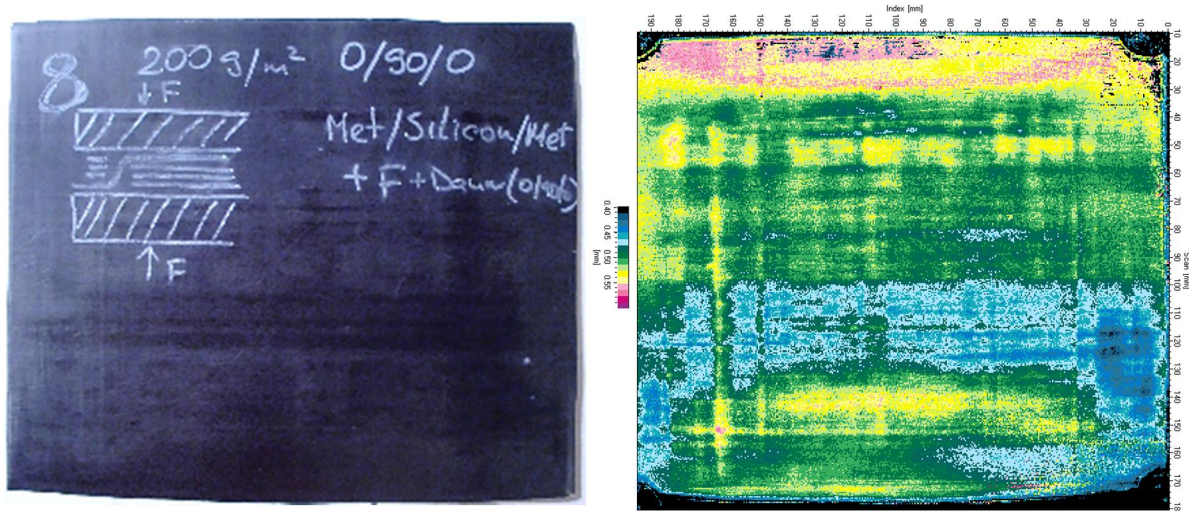


Figure 2.8. Panel VIII with corresponding US thickness scan

Specimen VIII represents three layer (200 g/m^2) panel compressed by pressure clamps (no vacuum bag applied for debulking), thick steel caul plates at the top and bottom were used. 1 mm silicon film layer were placed between upper caul plate and laminate with the reason to eliminate fibre bridging. Laminate was placed between steel plates, with dam formed by the same lay-up pre-preg 5 – 7 mm ribbons cut from the same panel. It should be noted that dam pre-preg ribbons was placed on the outside of the silicon film, so small amount of resin loss was observed. NDT scan showed good thickness distribution across the panel (except different thickness strips associated with pre-preg layer thickness variation) and some definite thickness difference, splitting panel horizontally in the middle (possibly associated with some thickness drop within single pre-preg layer or even multiplying (overlying) of those faults over two 0 layers, good compaction was observed, void spots was completely eliminated across all the panel (see Figure 2.8.). Thickness of the single ply measured for small panels was detected for two different thickness pre-preg as 0.09 mm (100 g/m^2) and 0.15 mm (200 g/m^2).

2.3 Face skin panel manufacturing

Mechanical compression was chosen as a final skin manufacturing method, based on preliminary panel manufacturing campaign, as most successful in terms of laminate compaction (void content) and thickness uniformity. Simple mechanical clamping device, see Figure 2.9. In addition, Figure 2.10. was designed and manufactured. Device consists of five parallel press frames manufactured from 25 x 30 mm C45 steel bars, connected by M10 bolts. Two rows of M16 bolts equipped with ballpoints facilitate clamping action on 10 x 60 mm steel ribbons that redistribute pressure on upper tool plate. Two steel plates, bottom tool plate (15 mm thick) and top tool plate (10 mm thick) was grind machined to facilitate precise mating planes. Both plates with internal silicon rubber layer atop pre-preg laminate lay-up, were used inside clamping device for forming of laminate skin plates. Silicon rubber sheet was necessary to compensate for variation of the thickness of the individual pre-preg layers. Direct placement of the pre-preg between tool plates (considering particular

pre-preg material) showed presence of low-pressure areas in close proximity to crossed thicker portions of pre-preg layers, see Figure 2.5. and Figure 2.6.

Henkel Frekote release agent was used for tool plates. First use treatment of application of 3 consecutive layers of Frekote release agent and followed heating of tool plates up to 150°C temperature was done. One layer of Frekote treatment done after each release to maintain release properties.

Typical curing cycle consisted of preheating the whole set-up up to resin flow state at 80°C withhold time for about 1 hour to allow entrapped air escape and resin to fill all cavities, followed by the rise of temperature up to 120°C withhold time of 3 hours to cure the resin to solid state with following gradual cooling to the room temperature in the oven left overnight.

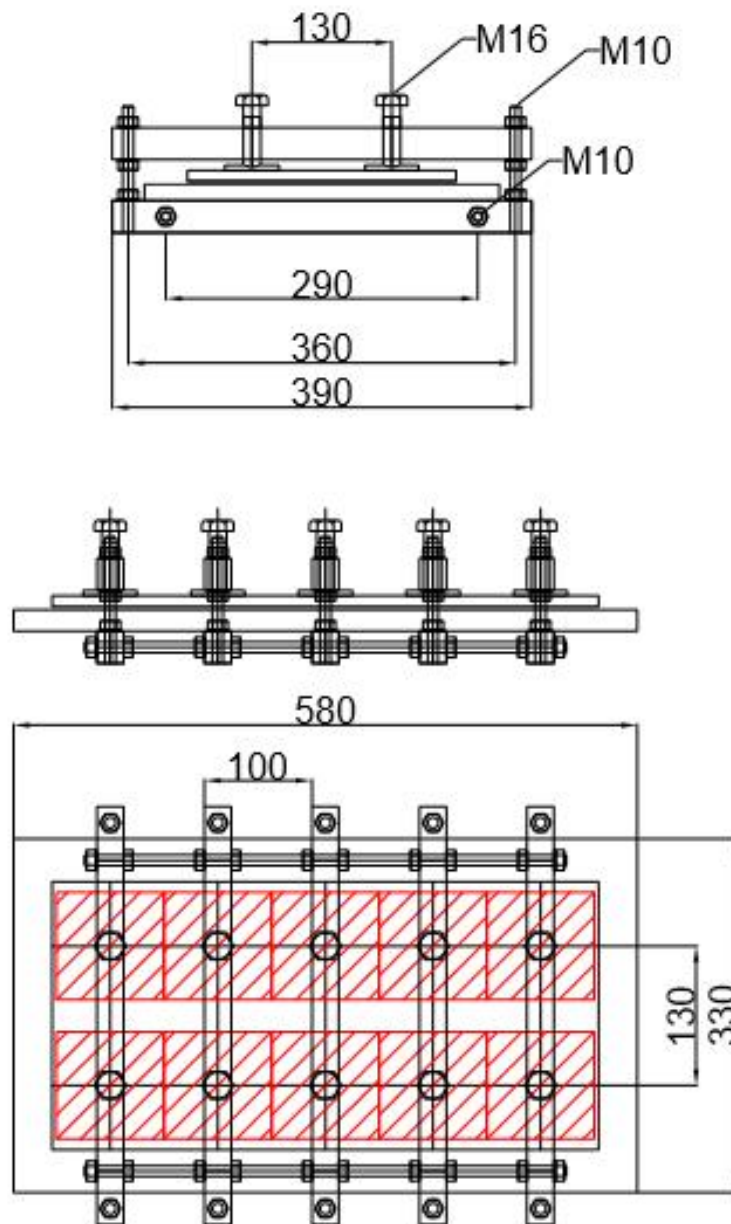


Figure 2.9. Mechanical clamping device for uniform pressure introduction.

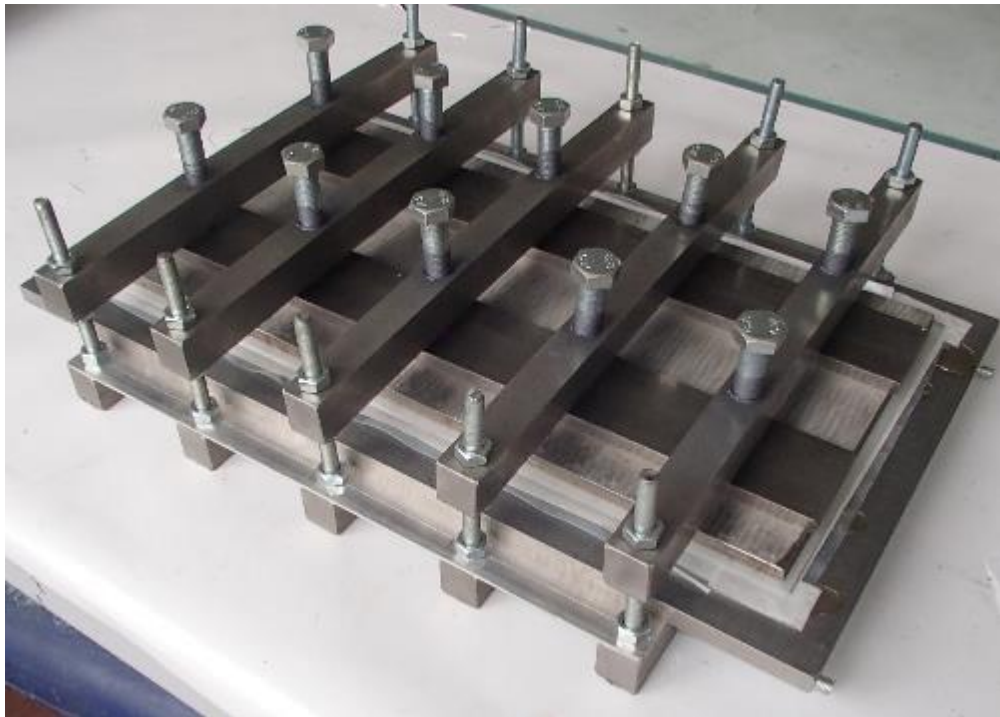


Figure 2.10. Mechanical clamping device for uniform pressure introduction.

Full size panels (480 x 220 mm) of different lay-ups were manufactured as preliminary studies. Two panels of 0/90/0 lay-up were manufactured of 100 g/m² and 200 g/m² pre-preg and was designated as Full panel 3 and Full panel 4 accordingly. Three more panels with +30/0/-30 lay-up Full panel 5 and +60/0/-60 lay-up Full panel 6 and Full panel 7, all manufactured from 100 g/m² pre-preg.

All full size panels were manufactured with the same technology, see Figure 2.11, as small panels during preliminary studies (Panel 7 and Panel 8), compression pressure introduced in clamping device by the dynamometric wrench was 10 N*m, which corresponds to total pressure introduced on plate of 39 kN or 0.31 Bar (0.31 N/mm²). 2 mm aluminium plate insert was used as upper caul plate for easier separation after curing. Laminate strips cut around the perimeter from the same plate lay-up was used as dam, separated by silicon rubber sheet from panel itself. The only drawback of this approach was that dam melting will occur just before plate melting and there is not enough pressure on the silicon film to hold all released resin from flowing out. Some kind of temperature resistant closed cell soft foam with slightly higher thickness than laminate should be used as dam to reduce resin loss at the panel edges.

Ultrasonic inspection of the full size panels was done. Ultrasonic thickness measurement bitmap image, accompanied with cross profile section for both axis and thickness histogram was shown on to Figure 2.16. Due to panel fixture restrictions, only (440 x 200 mm) part of the panel area was covered by US scan. Thickness calibration was performed for each particular panel by measuring thickness of the panel with calliper/micrometer at the one particular point near panel edge (marked on the panel surface). Speed of sound was adjusted to get ultrasound measured thickness value at the same marked point. That is why there is slight variation of speed of sound among the panels.

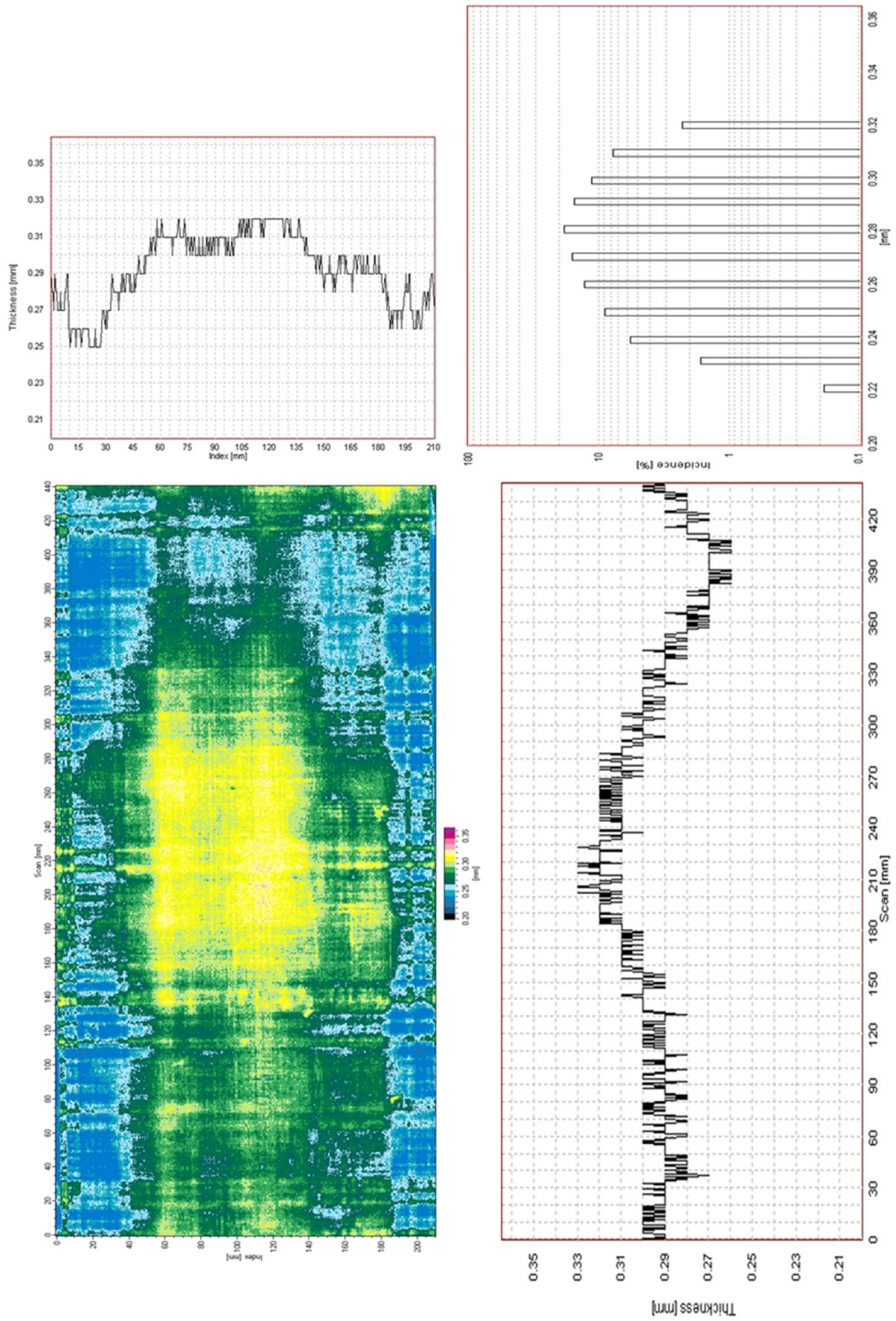


Figure 2.12. Full panel 3 (0/90/0) 100g/m²

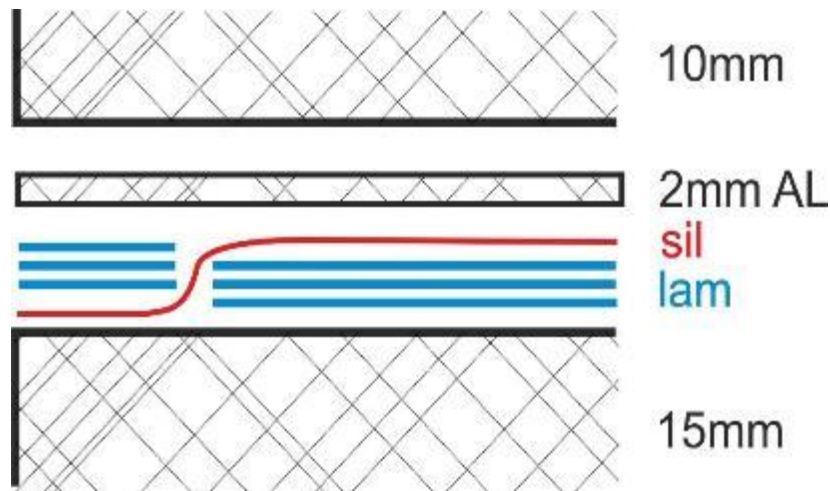


Figure 2.11. Laminate plate-manufacturing setup.

Average thickness of the panels was extracted from the thickness histogram as value with highest incidence, see Table 1. It should be taken into account that some panels have plato type histogram with fairly equal thickness incidences just above 10%, within 0.09 mm range (for 100 g/m² 3-ply panels), which equals to single layer thickness (about 30 % of overall panel thickness). Almost all panels have higher thickness at the centre of the panel and edges are thinner due to resin loss. Resin loss through the dam was still unresolved problem, since there is not vacuum bag used to hold resin flowing out of the edges of laminate. Such edge defects probably will make less impact on larger area panels or larger panels cured in vacuum bag and compressed in autoclave.

In-house created software for bitmap digitalization offer possibility to implement obtained thickness measurements into FE models or employs statistical analyses on thickness distribution, as well serves as reference measurement for impact damage characterization, but in general, serves as lamination quality measure, before sandwich assembly.

Table 2.1. Average measured thickness of full-scale panels.

Panel ID	Average panel thickness, mm	Average ply thickness, mm	Measured thickness range (1%≤incidences≤99%), mm	NDT speed of sound, m/s
Fullpanel 3	0.28	0.093	0.23 - 0.32	2000
Fullpanel 5	0.25 (0.28)	0.083 (0.093)	0.22 - 0.31	2000
Fullpanel 6	0.28	0.093	0.22 - 0.32	2000
Fullpanel 7	0.275	0.092	0.22 - 0.31	1950
Fullpanel 4*	0.52	0.173	0.44 - 0.63	-
* 200 g/m ² panel				

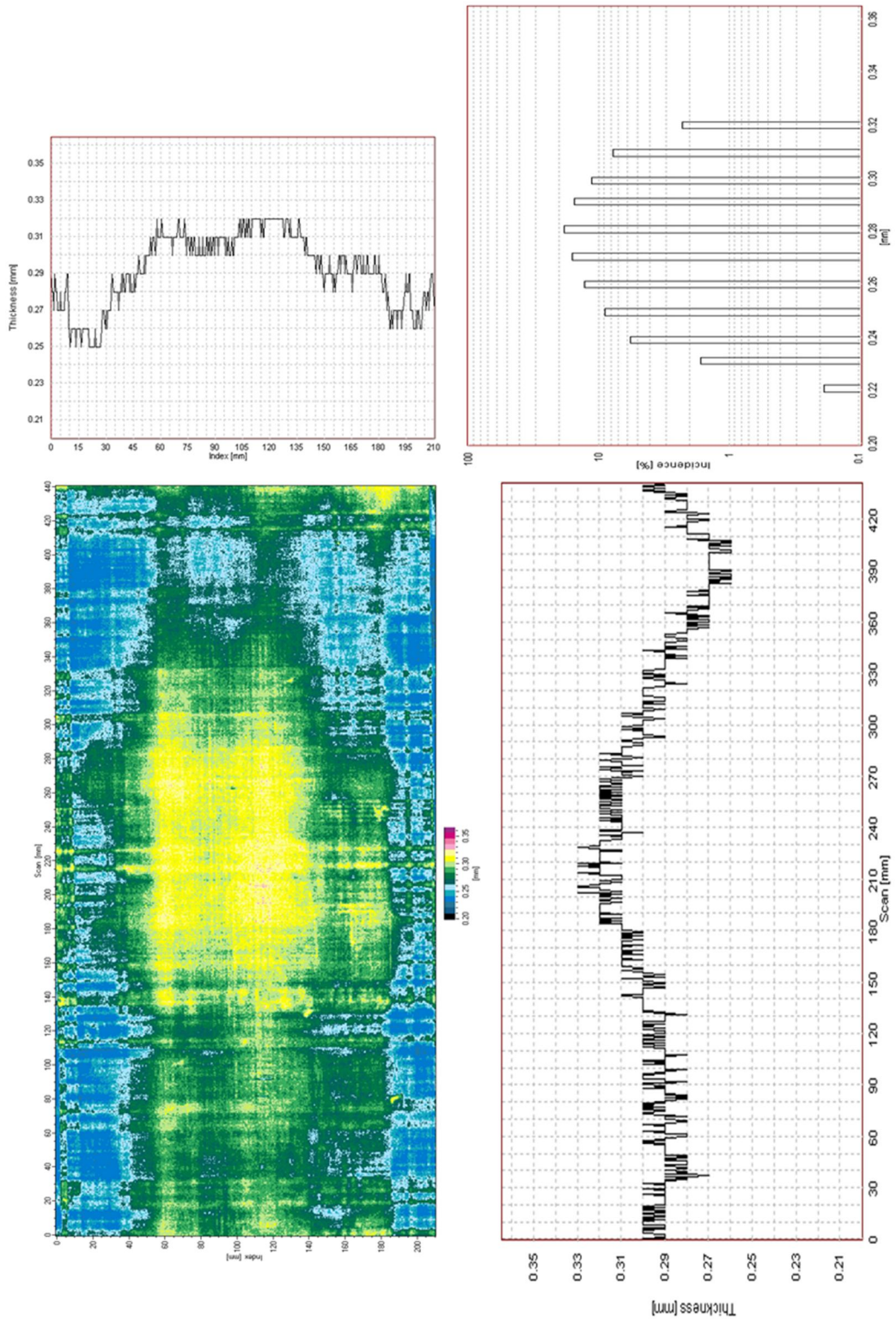


Figure 2.12. Full panel 3 (0/90/0) 100g/m²

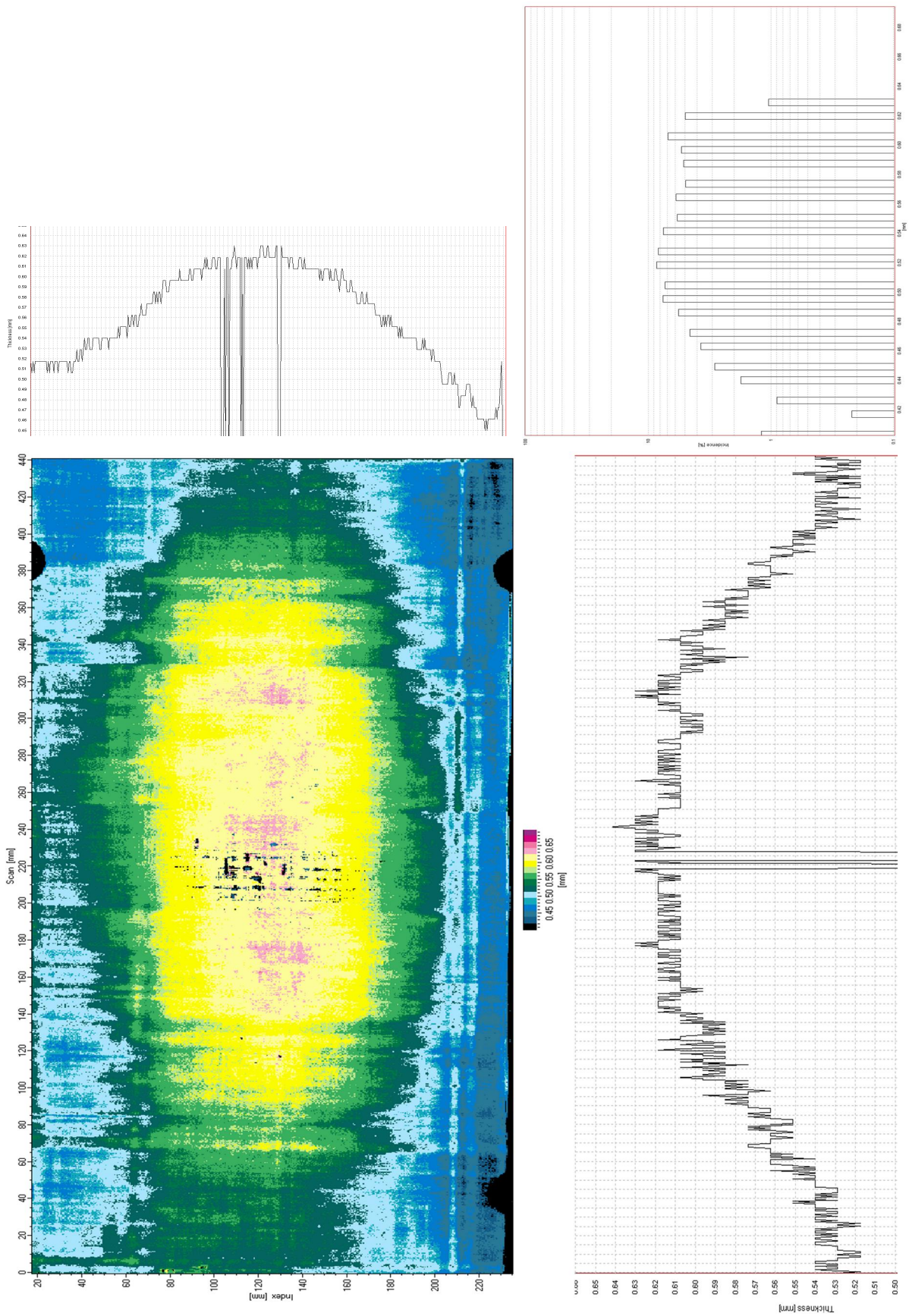


Figure 2.13. Full panel 4 (0/90/0) 200g/m².

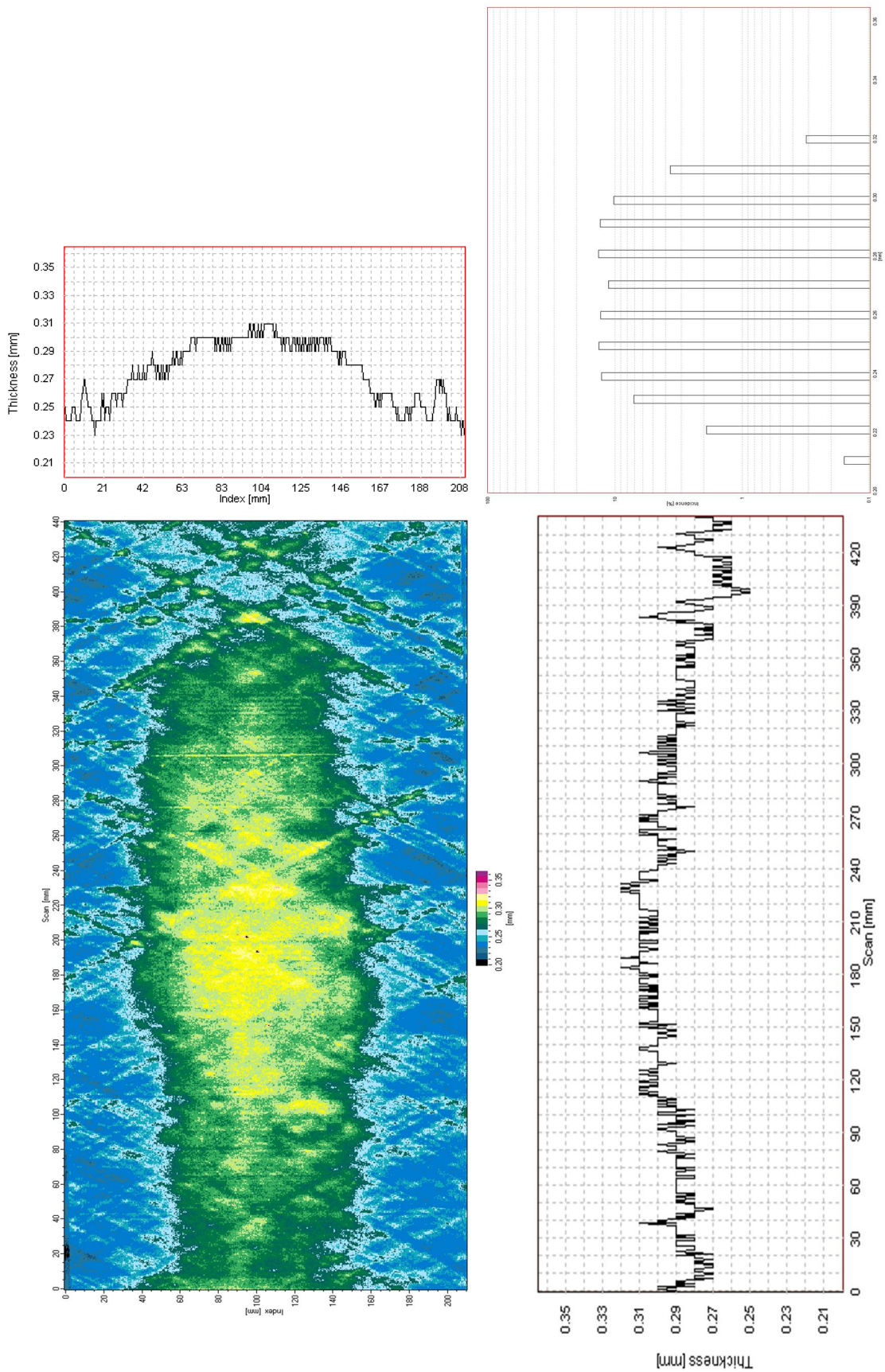


Figure 2.14. Full panel 5 (+30/0/-30) 100g/m².

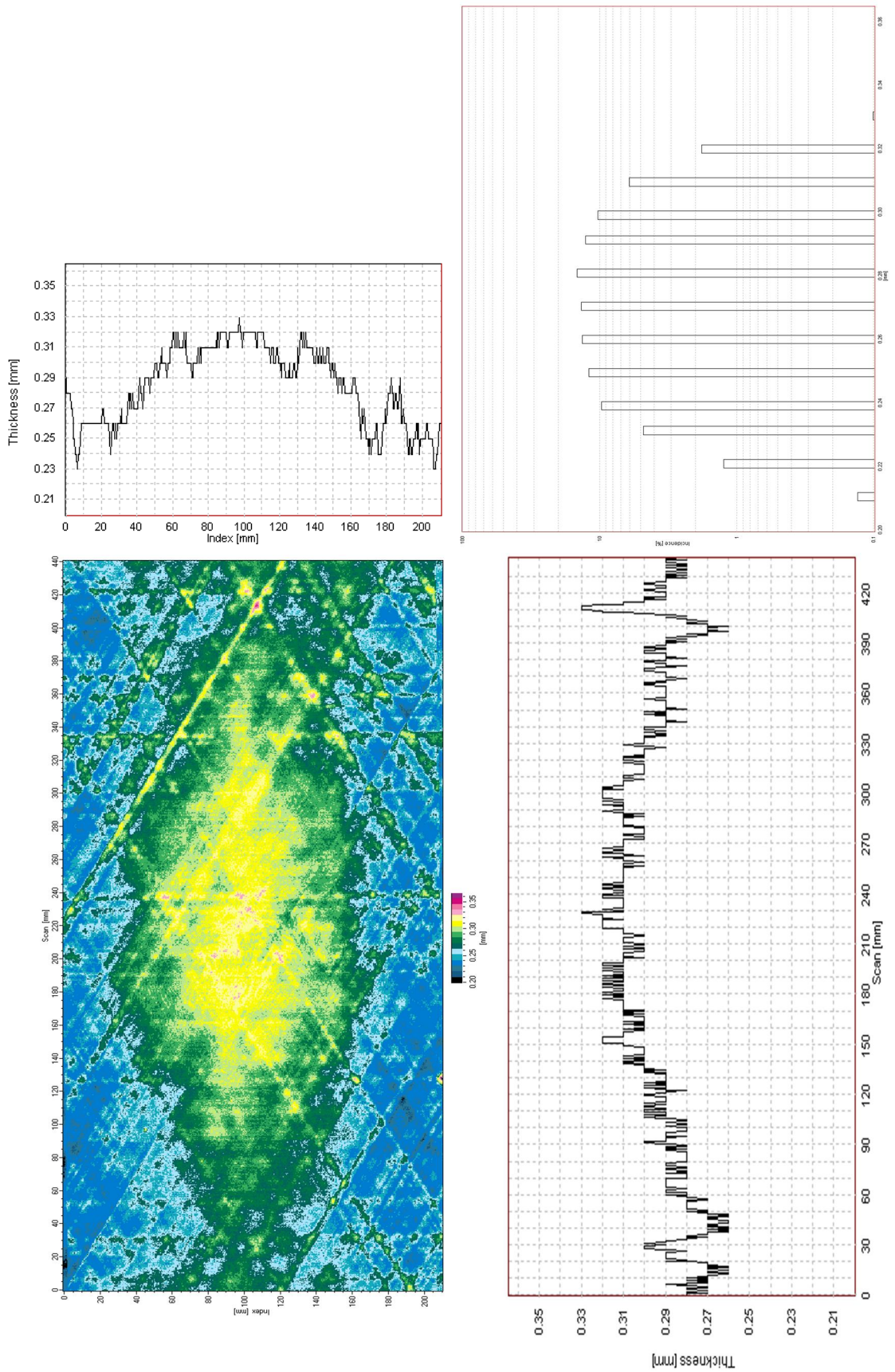


Figure 2.15. Full panel 6 (+60/0/-60) 100g/m².

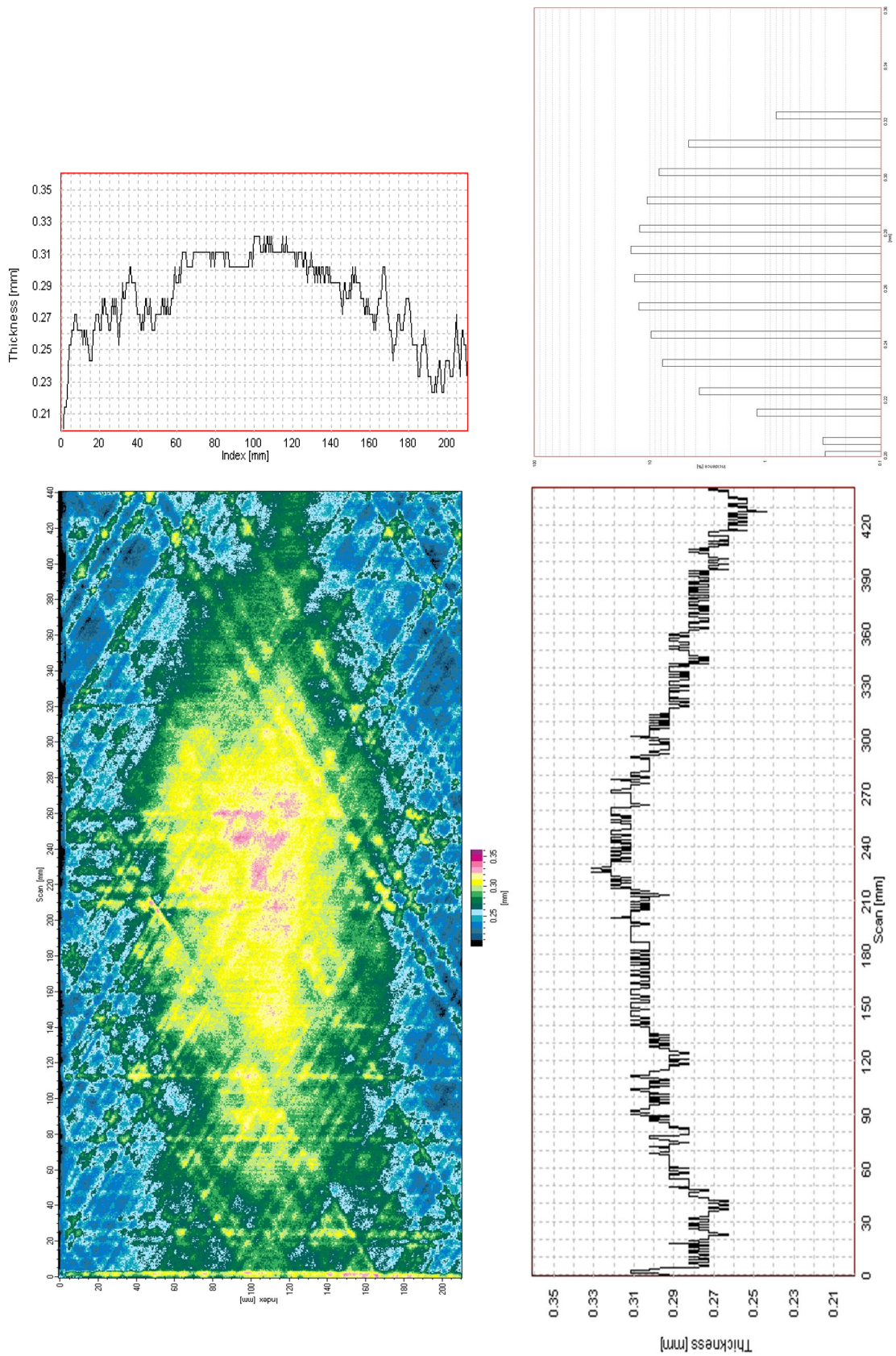


Figure 2.16. Full panel 7 (+60/0/-60) 100g/m².

2.4 Honeycomb preparation

Mostly aluminium honeycomb is supplied in sliced form (HOBE). Obviously, before sandwiching it between CFRP skins it is needed to expand. To achieve best results appropriate equipment should be used. Figure 2.17. shows custom made machine for HOBE expansion which in general is aluminium profile device with several pins to grab honeycomb's cells which are arranged along the fixed bar and along the moving bar to pull them for HOBE expansion. Moving bar moves along the guides on linear bearings. Pins inserted through the honeycomb edge cells arranged in pairs in an aluminium fork, see Figure 2.18. secured by bolt into aluminium profile groove, allowing for lateral movement during HOBE expansion. Paired pins provide better load distribution along the honeycomb edge, thus providing better-expanded cell geometry.

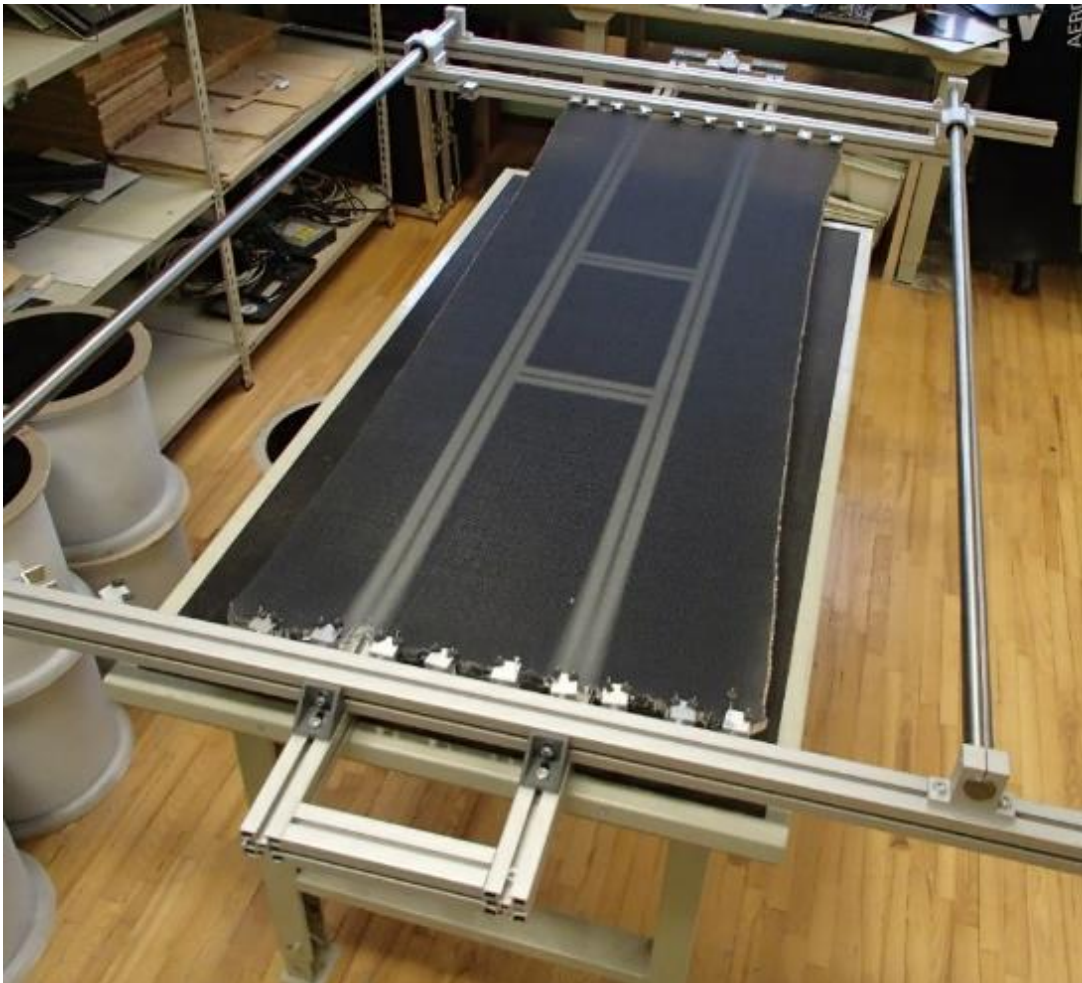


Figure 2.17. Honeycomb expansion machine.

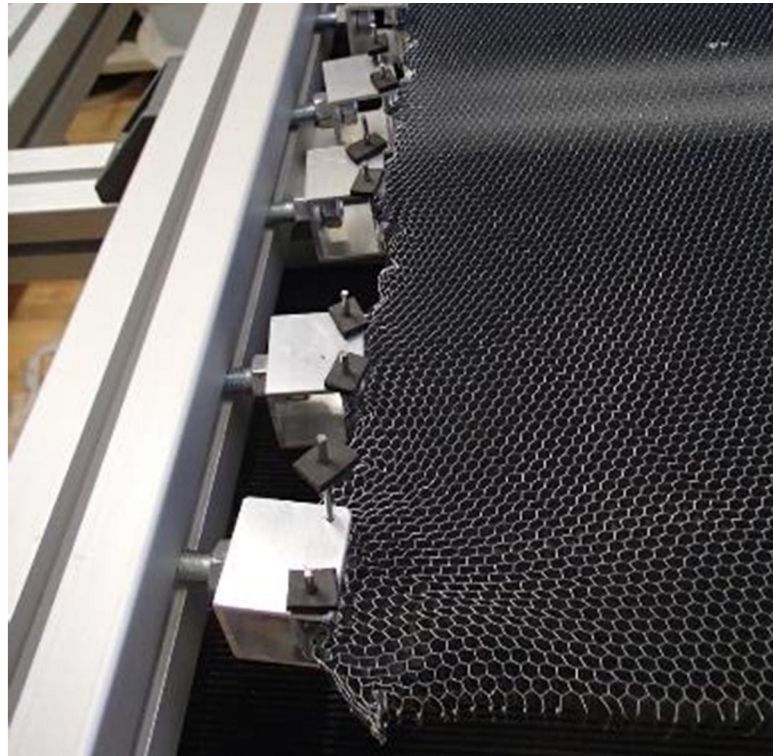


Figure 2.18. Pin hooked edge during honeycomb expansion.

Expanded honeycomb cell geometry can be monitored by means of cell geometry measurement during expansion, with micrometer measuring section of 10 cells, for example, or performing final geometry check by image comparison against ideal hexagonal mesh, see Figure 2.19.

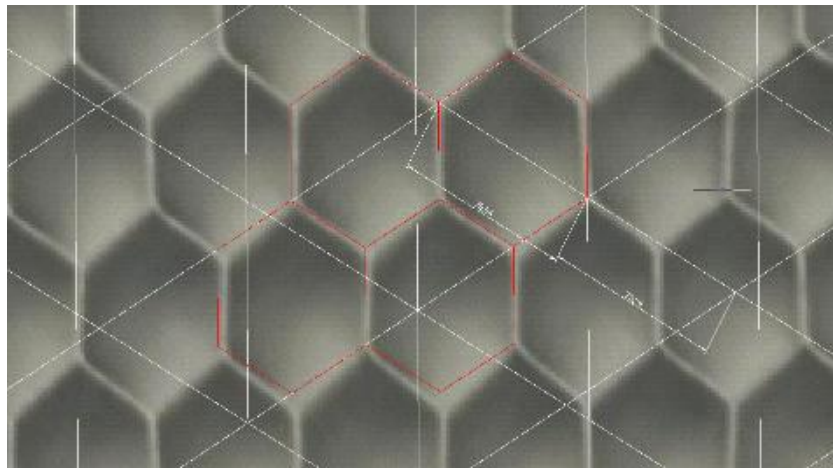


Figure 2.19. Honeycomb cell geometry comparison against perfect hexagonal.

Another one technique can be used by employing digital SLR camera equipped with pro quality telephoto lens with low barrel distortion at long end (CANON D40 + EF 70-200 f2.8L IS USM). Low ISO sensitivity (100 – 200 ISO) and small aperture f10 should be used along with sturdy tripod. Obtained images, see Figure 2.20., can be digitized by turning them into b/w high contrast image with filtered out black background, Figure 2.21. With the proper scaling, it is possible to convert bitmaps to xyz point cloud to process data digitally. The only limitation for this approach was DSLR

resolution, in this particular case 10 Mp sensor do not deliver sufficient pixel density to correctly capture honeycomb structure wall thickness, in other words honeycomb cell wall thickness was represented by one-pixel row. For better quality at least 24 Mp sensor camera should be used to represent honeycomb structure wall with at least two-pixel row.

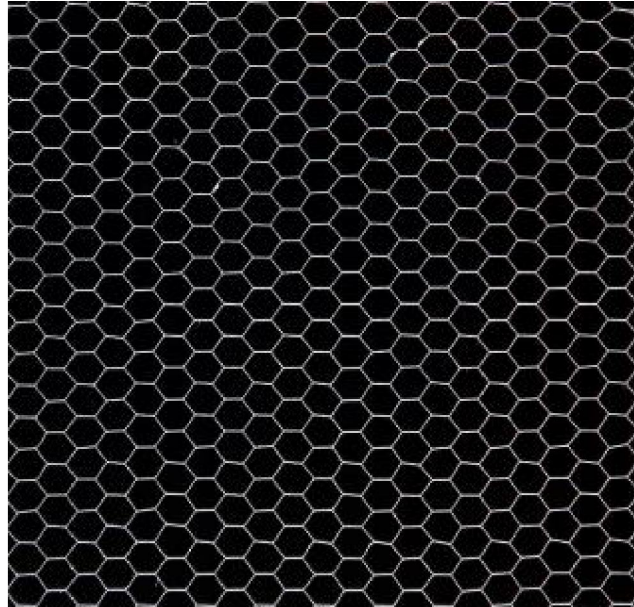


Figure 2.20. High contrast b/w image of honeycomb structure

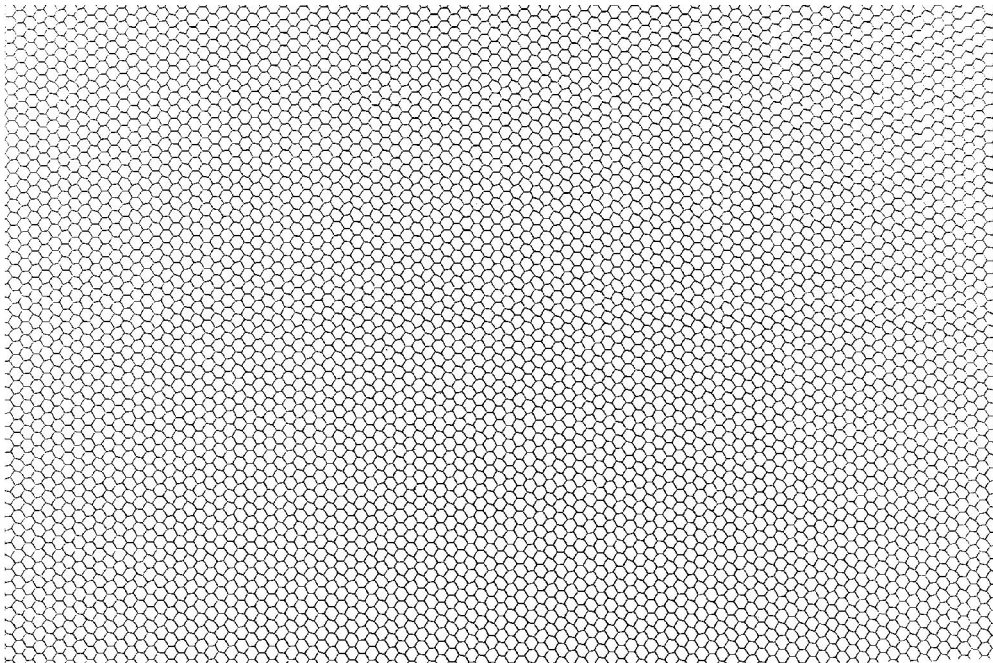


Figure 2.21. Approximate 300 x 200 mm panel structure image filtered from black background.

A dedicated equipment for barely visible impact damage assessed with laser distance meter mounted on US inspection machine manipulator replacing US probe, see Figure 2.22. US inspection software provides desired control over X-Y movement of the laser sensor over the surface of the measured panel, while actual X-Y

coordinates along the distance to the panel surface were measured and recorded by MGCplus data acquisition system. X and Y-axis coordinates was measured by draw wire sensors (DWS) with corresponding distance data, forming xyz point cloud of the measured surface, see Figure 2.23. Acquitted data can be transformed into contour plot with any math software available to represent indentation area and size, as well as, directly implemented into FE model. Since surface scanning process was heavily time consuming, further studies on scan density y across undamaged areas should be verified on first successful sandwich prototypes.

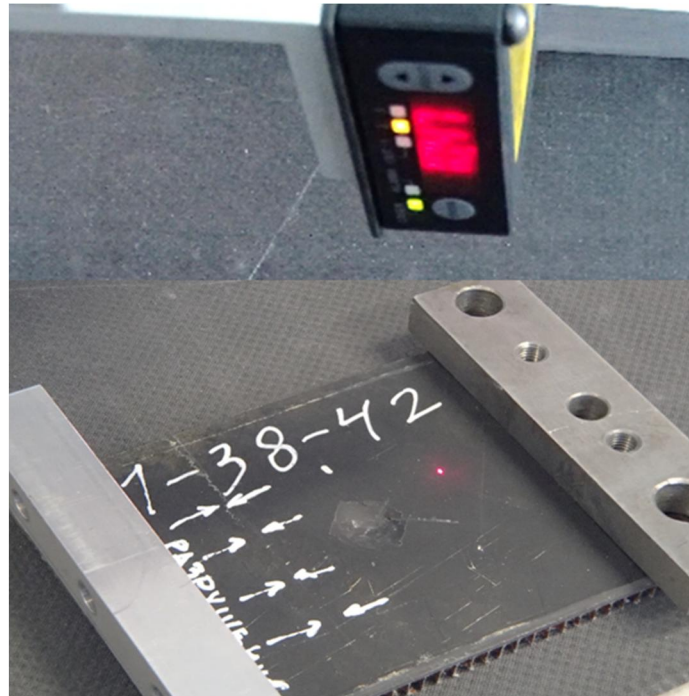


Figure 2.22. Surface imperfection measurement on scratch sample

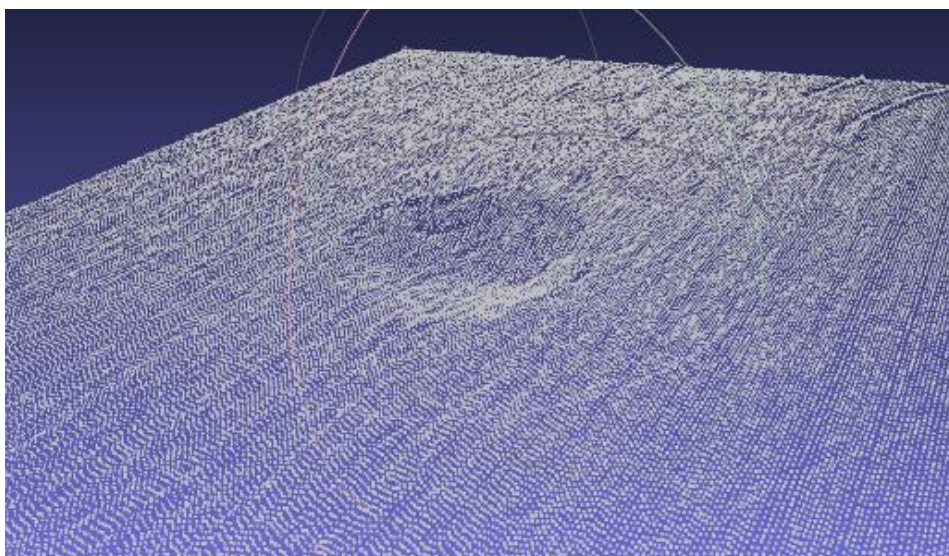


Figure 2.23. Indentation measurement xyz point cloud example.

2.5 Panel assembly

Two-stage panel assembly was considered as the only available due to necessity for compaction of face sheet laminate, produced of pre-preg UD layers, to produce composite plate with minimized porosity and highest possible stiffness. In general, panel-assembling process presented on Figure 2.24. represent adhesive bonding of aluminium honeycomb core between two composite laminate face sheets. Different types of adhesives are in use for panel assembly, the most widely used is film adhesive assembly. During preliminary studies, panels were assembled with 2C PUR two component polyurethane adhesive, which showed good adhesion capabilities both to aluminium and carbon fibre composite. Due to tendency to flow before PU, setting the completely boning procedure was divided into separate bonding of each of the face sheets, to avoid resin gravity flow away from the upside down positioned upper face sheet.

Preliminary studies showed that epoxy resin has not enough adhesion to the aluminium to withstand out of plane forces to be used as bonding adhesive, with the exclusion to high ductility (hardened) epoxies usually found in film structural adhesives.

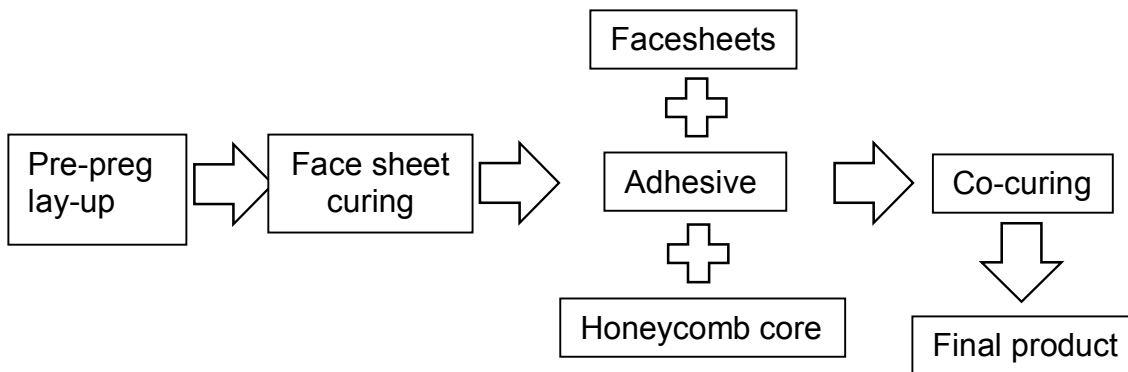


Figure 2.24. Two step panel assembly

3 Experimental procedures

This report does not contain standard test procedures on characterization of mechanical properties of UD carbon fibre laminates, but mainly focused on sandwich structure test procedures. The basic honeycomb core and sandwich panel tests are contained in ASTM Standards Test Methods Volume 15.03 (Space Simulation, Aerospace and Aircraft, High Modulus Fibers and Composites) and the Military Standard 401B (Sandwich Constructions and Core Materials). Also, all the major aircraft companies have their own internal honeycomb specification requirements [1], for example, SACMA SRM 2-88, NASA 1 092, Composites Research Advisory Group (CRAG), Boeing and others.

The relatively complex structure of honeycomb sandwich panel and variety of test methods makes difficulties to create simple and understandable framework of all methods to be logically divided into groups. There is need to review all standards which are related to honeycomb sandwich panels and for its separate components (facings and core) and finally to develop method for damaged panel's residual strength estimation, because, as mentioned before, so far there is not any. Test methods, more or less connected to topic of this review are collected in flowchart shown in Figure 3.1.

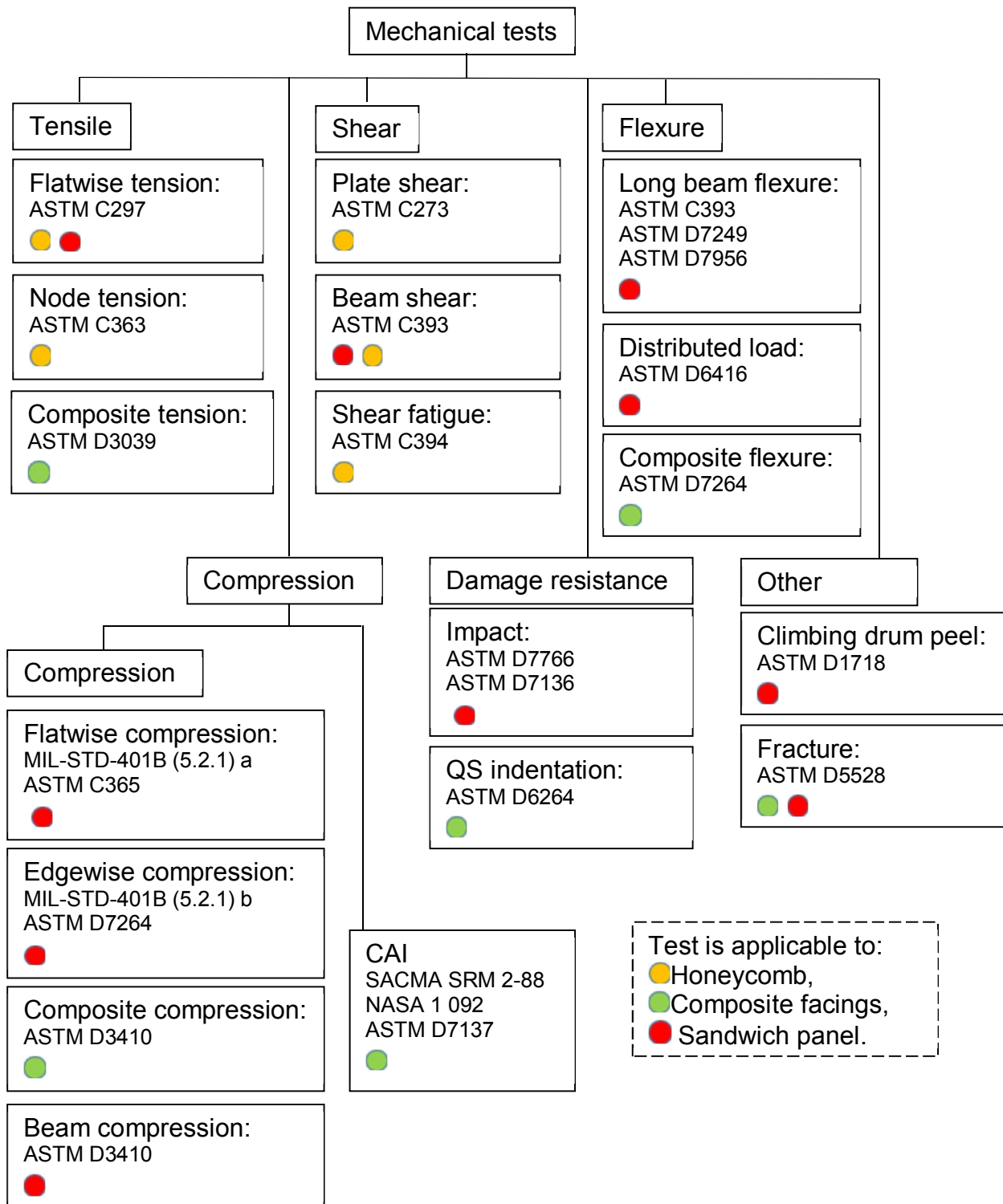


Figure 3.1. Test methods related to CFRP/honeycomb sandwich damage tolerance estimation

3.1 Non-destructive testing – Modal assurance criterion

3.1.1 Introduction to Modal assurance criterion

One of the most popular tools for the quantitative comparison of modal vectors is the Modal Assurance Criterion (MAC). The development of the MAC was modelled after the development of the ordinary coherence calculation associated with computation of the frequency response function. The MAC is a statistical indicator, just like ordinary coherence. This least squares based form of linear regression analysis yields an indicator that is most sensitive to the largest difference between comparative values and results in modal assurance criterion that is insensitive to small changes or small magnitudes. The MAC was originally introduced in modal testing in connection with The Modal Scale Factor, as an additional confidence factor in the evaluation of modal vector from different excitation locations. When an FRF matrix is expressed in the partial fraction expansion form, the numerator of each term represents the matrix of residues or modal constants [2].

The MAC is calculated as the normalized scalar product of the two sets of vectors $\{\varphi_A\}$ and $\{\varphi_X\}$. The resulting scalars are arranged into the MAC matrix:

$$MAC(r, q) = \frac{|\{\varphi_A\}_r^T \{\varphi_X\}_q|^2}{(\{\varphi_A\}_r^T \{\varphi_A\}_r) (\{\varphi_X\}_q^T \{\varphi_X\}_q)}$$

Where the form of coherence function can be recognized, indicating the casual relationship between φ_A and $\{\varphi_X\}$.

3.1.2 Modal Assurance Criterion presentation formats

One of the big changes in the application of the MAC over the last years in the way the information is presented. Today most computer systems routinely utilize colour to present magnitude data like MAC using 2D and 3D plot, see Figure 3.2. It is important to remember that MAC is a discrete calculation and what appears as a colour contour plot really only represents the discrete mode-to-mode comparison. Nevertheless, a colour plot does allow more data to be presented in an understandable form in minimum space.

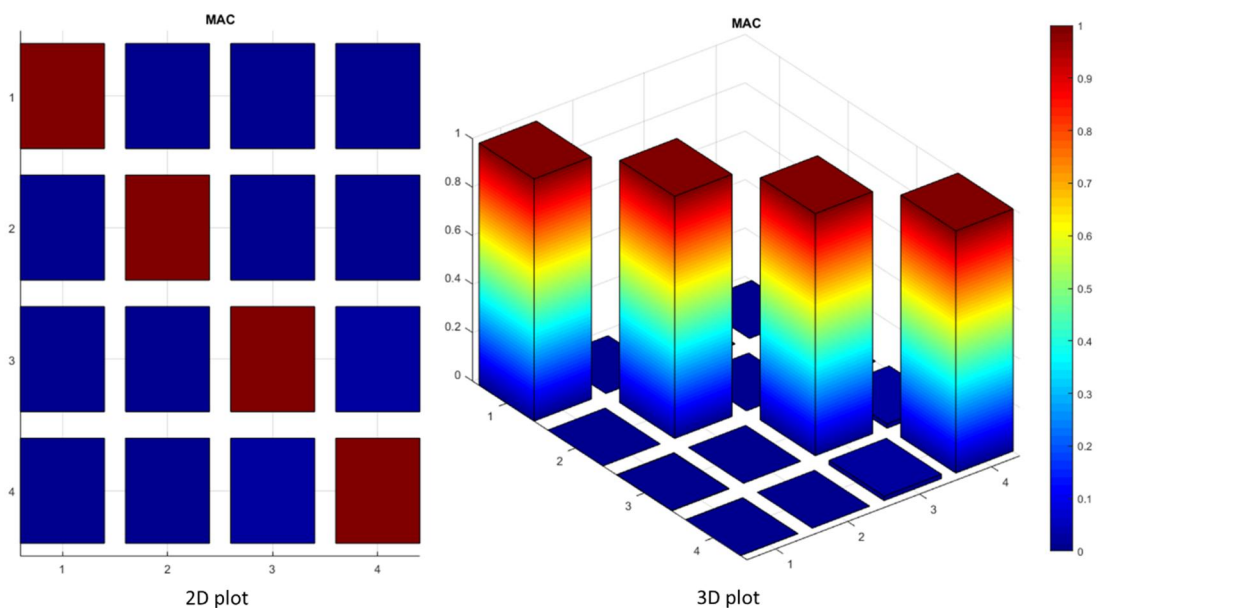


Figure 3.2. MAC plot example.

3.1.3 Modal Assurance Criterion (MAC) Zero.

If the modal assurance criterion has a value near zero, this is an indication that the modal vectors are not consistent. This can be due to any of the following reasons:

- The system is non-stationary. This can occur if the system is nonlinear and two data sets have been acquired at different times or excitation levels. System nonlinearities will appear differently in frequency response functions generated from different exciter positions or excitation signals. The modal parameter estimation algorithms will also not handle the different nonlinear characteristics in a consistent manner.
- There is noise on the reference modal vector. This case is the same as noise on the input of a frequency response function measurement. No amount of signal processing can remove this type of error.
- The modal parameter estimation is invalid. The frequency response function measurements may contain no errors but the modal parameter estimation may not be consistent with the data.
- The modal vectors are from linearly unrelated mode shape vectors. Hopefully, since the different modal vector estimates are from different excitation positions, this measure of inconsistency will imply that the modal vectors are orthogonal. If the first four reasons can be eliminated, the modal assurance criterion can be interpreted in a similar way as an orthogonally calculation.

3.1.4 Modal Assurance Criterion (MAC) Unity.

If the modal assurance criterion has a value near unity, this is an indication that the modal vectors are consistent. This does not necessarily mean that they are correct. The modal vectors can be consistent for any of the following reasons:

- The modal vectors have been incompletely measured. This situation can occur whenever too few response stations have been included in the experimental determination of the modal vector.
- The modal vectors are the result of a forced excitation other than the desired input. This would be the situation if, during the measurement of the frequency response function, a rotating piece of equipment with an unbalance is present in the system being tested.
- The modal vectors are primarily coherent noise. Since the reference modal vector may be arbitrarily chosen, this modal vector may not be one of the true modal vectors of the system. It could simply be a random noise vector or a vector reflecting the bias in the modal parameter estimation algorithm. In any case, the modal assurance criterion will only reflect a consistent (linear) relationship to the reference modal vector.
- The modal vectors represent the same modal vector with different arbitrary scaling. If the two modal vectors being compared have the same expected value when normalized, the two modal vectors should differ only by the complex valued scale factor, which is a function of the common modal coefficients between the rows or columns.

3.1.5 Experimental procedure and results

The **Polytec PSV-400 Vibrometer** is an innovative measurement tool for non-contact measurement, visualization and analysis of structural vibrations. It determines the operational deflection shapes and Eigen modes as easily as taking a photograph.

Entire surfaces can be scanned automatically using flexible and interactive measurement grids. Measurements can be made over a wide frequency bandwidth. The PSV-400 offers technical excellence with powerful software for dynamic measurement, analysis and real-time chromatic display of data. Designed for resolving noise and vibration issues in R&D and manufacturing, the system is versatile and easy to use. Additional test machine parameters are given in table 2. All tests were performed at a temperature of 20-22° Celsius and relative air humidity of 33-35%.

Basing on frequency response graph (Figure 3.3) also is possible to estimate quality of the specimen. For example, large amount of noise on response graph

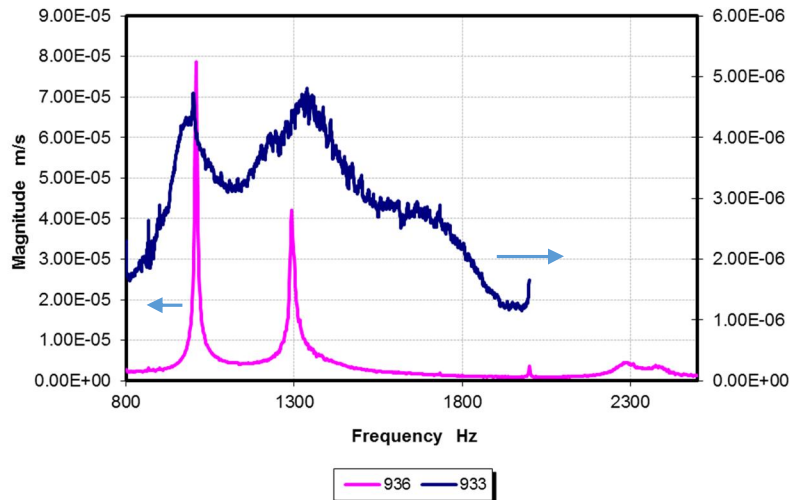


Figure 3.3. Frequency response graph

Using frequency response graph (Figure 3.3.) it is possible to estimate the quality of the specimen. If there is a large amount of noise in received response, one of the factors of this phenomenon may be a bad connection between the sandwich components and this was sustained by climbing drum peel test and flatwise tension of the panel.

Continuing modal analysis investigations of sandwich plates it was found that specimens ESA 001 to ESA 004 are almost identical to each other and this is shown by frequency response with minimal divergence (Figure 3.4.).

Using modal assurance criterion technique for quality control and sensitivity analysis between modes were obtained MAC. Obtained modal assurance criterion plots are shown in Figure 3.5

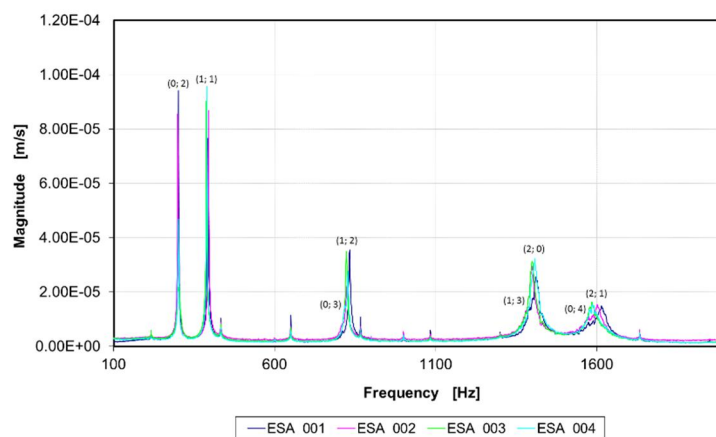


Figure 3.4. Frequency response

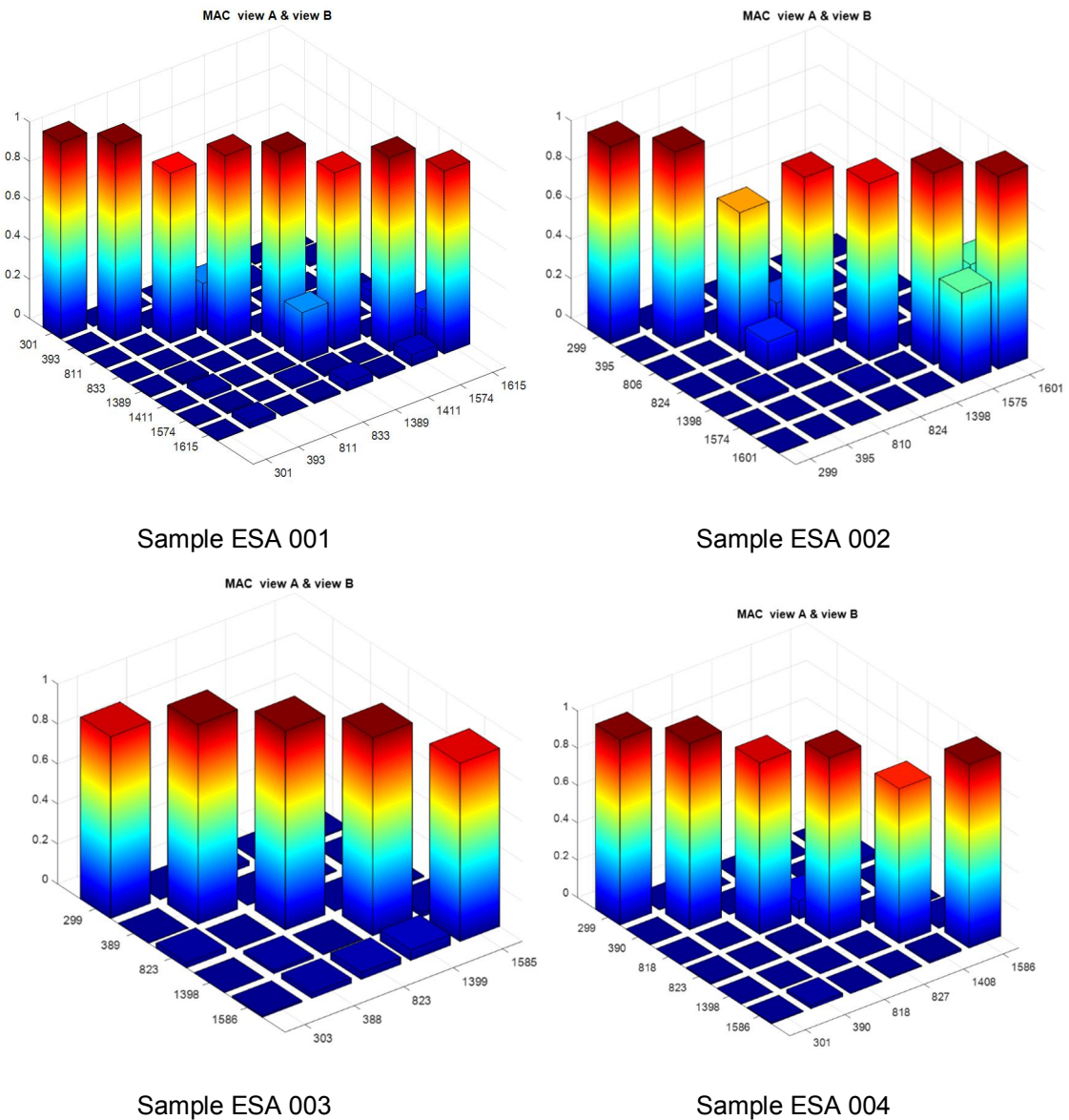


Figure 3.5. Modal assurance criterion plot

3.1.6 Conclusions

A current report summarises effort given for setting up a manufacturing procedures for prototyping of CFRP/Al-honeycomb panels. Currently four panels with 480 x 220 have been produced and non-destructively evaluated by ultrasound and vibration methods. It has been recognized that thickness distribution, low porosity and stiffness has been achieved in accordance with highest standards of composite production. A continuous production of sandwich panels are foreseen in upcoming period.

4 References

1. Allemang, R. J., "Investigation of Some Multiple Input/Output Frequency Response Function Experimental Modal Analysis Techniques," Doctor of Philosophy Dissertation, University of Cincinnati, Department of Mechanical Engineering, pp. 141-214, 1980.
2. Allemang, R. J., Brown, D. L., "A Correlation Coefficient for Modal Vector Analysis," Proceedings, International Modal Analysis Conference, pp. 110-116, 1982.
3. Fotsch, D., Ewins, D., J. Application of MAC in the Frequency Domain, Mechanical Engineering Department, Imperial College of Science, Technology and Medicine, London, UK .
4. Avilés, R. 2009, The Modal Assurance Criterion (MAC). Bilbao.